Functionalized chitosan biosorbents with ultra-high performance, mechanical strength and tunable selectivity for heavy metals in wastewater treatment

Functionalized chitosan biosorbents with ultra-high performance, mechanical strength and tunable selectivity for heavy metals in wastewater treatment

Bingjie Wang, Yong Zhu, Zhishan Bai, Rafael Luque, Jin Xuan

PII: S1385-8947(17)30814-8
DOI: http://dx.doi.org/10.1016/j.cej.2017.05.065
Reference: CEJ 16963

To appear in: *Chemical Engineering Journal*

Received Date: 11 March 2017
Revised Date: 8 May 2017
Accepted Date: 9 May 2017

Please cite this article as: B. Wang, Y. Zhu, Z. Bai, R. Luque, J. Xuan, Functionalized chitosan biosorbents with ultra-high performance, mechanical strength and tunable selectivity for heavy metals in wastewater treatment, *Chemical Engineering Journal* (2017), doi: http://dx.doi.org/10.1016/j.cej.2017.05.065

Functionalized chitosan biosorbents with ultra-high performance, mechanical strength and tunable selectivity for heavy metals in wastewater treatment

BingjieWang[a,b], Yong Zhu[a], ZhishanBai[a*], Rafael Luque[b*], Jin Xuan[c*]

[a] *State Environmental Protection Key Laboratory of Environmental Risk Assessment and Control on Chemical Process, School of Mechanical and Power Engineering, East China University of Science and Technology, Shanghai 200237, PR China*

[b] *Departamento de Quimica Organica, Universidad de Córdoba, Campus de Rabanales, Edificio Marie Curie (C-3), Ctra Nnal IV-A, Km 396, Córdoba, E14014, Spain*

[c] *School of Engineering and Physical Sciences, Heriot-Watt University, Edinburgh, EH14 4AS, United Kingdom*

[*]*Corresponding Authors, Email addresses:* q62lsor@uco.es *(R. Luque),* baizs@ecust.edu.cn *(Z. Bai),* j.xuan@hw.ac.uk *(J. Xuan). Tel: +44 (0) 131 451 3293; Fax: +44 (0)131 451 3129.*

ABSTRACT

Water pollution is the most challenging issue facing mankind nowadays as a result of ever-increasing population and steadily improving life standards. More and more wastewater without effective treatments is arbitrarily discharged into the aquatic environment, which causes irreversible damage and incalculable loss. Especially, the industrial wastewater containing heavy metal ions, such as copper (Cu), cobalt (Co), and manganese (Mn), are toxic to human and living organisms even at low concentrations. A highly efficient and selective removal method has been long sought for heavy metal ions wastewater treatment. In this study, a highly monodispersed polyethylenimine-chitosan (PEI-CS) biosorbent, synthesized by an integrated process with facile microfluidic emulsion, chemical crosslinking,

solvent extraction and chemical modification, was used as an efficient adsorbent to remove heavy metal ion from contaminated water. The as-prepared biosorbents demonstrated ultra-high adsorption capacity of 146 mg g^{-1} towards Cu ions, almost triple the performance reported in literature. Besides, PEI-CS biosorbents were also endowed with good mechanical strength, excellent adsorption selectivity towards targeted ion in the presence of other metal ions with different valence states, and high reusability. Therefore, the newly developed PEI-CS biosorbents is a highly promising candidate for wastewater treatment with heavy metal ions.

Keywords: Wastewater treatment; heavy metal adsorption; microfluidics; chitosan biosorbents; polyethylenimine functionalization.

1. Introduction

With the rapid development of the economy and the lasting improvement of the modernization, large quantities of wastewater containing complex multi-components have become an ecotoxicological hazard. Especially, heavy metal contaminants, distinguished from organic pollutants[1], can hardly be biodegraded and will gradually accumulate in living organisms which may cause serious environmental and health problems[2-5]. Untreated and partially treated wastewater from agriculture (redundant fertilizers and pesticides), metallurgy (mining and smelting) and energy sectors (power plants and battery manufacture) currently containing several heavy metal ions is directly discharged into aquatic environments which contributed significantly to such severe ecological and environmental issues[6].Toxic metals including Co, Mn, and Cu pose serious and irreversible damages to human beings such as nervous system disorders, chronic and acute poisoning and the loss of organ functions[7-9].

The elimination of toxic metal ions from contaminated water prior to discharge is consequently in great demand. Various approaches including chemical precipitation[10], electrochemical reaction[11], membrane filtration[12-16], ion-exchange[17, 18], reverse osmosis and adsorption[19-22] have been established for wastewater treatment. Among them, adsorption emerged as the most promising method due to its versatility, wide applicability, economic feasibility, and low toxic with no by-products generation[23-31].

Natural sorbent sand bio-sorbents including activated carbon[32] and chitosan[33, 34] are widely available at low cost but they usually exhibit non-selective adsorption capacities and poor mechanical properties. On the other hand, engineered (nano)materials[35-37] (i.e. polymers) have demonstrated superior adsorption performance with controllable properties but always associated with much higher cost and a larger environmental footprint. In this study, an advanced strategy to engineer biosorbents has been developed aiming to combine advantages from both natural and engineered materials. A new biosorbent based on chitosan was synthesized using a facile and reliable targeted surface modification and functionalization process, showing outstanding advantages of cost-competitiveness, efficiency and reliability in heavy metal wastewater treatment applications.

Chitosan (CS), originated from chitin deacetylation is the unique alkaline polysaccharide and widely distributed second only to cellulose in the natural world, exhibiting various excellent physicochemical properties including being nontoxic, biocompatible and biodegradable[38, 39]. However, chitosan is very sensitive to environmental pH change and can easily form gels or dissolve in wastewater, which hinders its practical applications[40]. With the rapid development of microfluidic technology, chitosan crosslinked microparticles derived from microfluidic emulsions have been recently reported as promising heavy metal adsorption materials[41, 42]. The precise control of particle morphology featured with highly monodispersed, controllable sizes and various

structures provides CS biosorbents with additional adsorption capacity and robustness. However, the microfluidic platform still fails to produce optimum sorbents for selective adsorption of heavy metals. To date, the highest heavy metal (Cu^{2+}) adsorption capacity for microfluidically synthesized CS biosorbents was reported to be 52 mg g^{-1} [42], with large room for further improvements. Moreover, no work has been done so far to study the mechanical strength of microfluidic-synthesized adsorbents to fulfill the requirement of practical industrial processes, especially, in consideration of balancing mechanical strength with adsorption capacity. Besides, there is also a lack of the exploration to the adsorption mechanism and performance optimization for selectivity and reusability.

To fulfill this research gap, a facile engineering process integrating chemical crosslinking, solvent extraction and functional group grafting has been developed in this study to realize the performance optimization base on microfluidic emulsion. We successfully synthesized highly monodispersed PEI-CS biosorbents (CV < 2.5%) based on the newly developed integrated process (Fig. 1). The new functionalized biosorbents are featured with ultra-high adsorptive performance (146 mg g^{-1}) towards Cu ions, which was almost triple the best literature reported performance (52 mg g^{-1}) for CS biosorbents [42]. It also exhibited an unprecedented mechanical strength (0.34 MPa), comparable with commercial artificial polymers and superior to most natural sorbent materials. The PEI-CS biosorbents also show an excelling selectivity (up to 94.7 %) towards targeted Cu ions and outstanding regeneration properties.

2. Experimental section

2.1 Materials

The starting material was medium molecular weight chitosan (85 % deacetylated), purchased from Aladdin-Biochemical Technology Co., Ltd. *n*-Octane, *n*-octanol, acetone,

epoxy chloropropane and isopropyl alcohol were purchased from Lingfeng Chemical Reagent Co., Ltd., without further purification. Ethanol was purchased from Titan Scientific Co., Ltd. Polyethylenimine (PEI) solution (50 %) was purchased from Sigma-Aldrich. Span 80, acetic acid, ethylene diamine tetraacetic acid (EDTA), $CuCl_2 \cdot 2H_2O$, $CoCl_2 \cdot 6H_2O$, $MnCl_2 \cdot 4H_2O$, NaCl, and $AlCl_3 \cdot 6H_2O$ were purchased from Sinopharm Chemical Reagent Co., Ltd. All metal ion solutions were prepared in deionized water. Glutaraldehyde (50 %) was purchased from Aladdin-Biochemical Technology Co., Ltd. Glutaraldehyde was pre-extracted under *n*-octanol to obtain the glutaraldehyde saturated *n*-octanol solution at room temperature for 10 h before use. All reagents were analytical grade and used as received. Deionized distilled water was used throughout the experiments.

2.2 Biosorbent synthesis

2.2.1 CS biosorbents

The synthesis process of CS biosorbents is schematically shown in Fig. 1a. An aqueous polymer solution prepared by adding 4 wt% chitosan in 2 wt% acetic acid was used as the dispersed phase in our experiments to synthesize chitosan emulsion templates. The dispersed phase was continuously stirred until chitosan was thoroughly dissolved, and utilized after several filtrations and vacuum degassing. The continuous phase was *n*-octanol added with 2 wt% Span 80 serving as stabilization. Via adjusting the velocities of continuous phase and dispersed phase, a series of chitosan emulsion templates with a certain size were firstly generated at the flow-focusing geometry of a microfluidic chip (see SI Fig. S1) under the shearing force from both sides. 0.5 wt% Glutaraldehyde saturated *n*-octanol solution mixed with *n*-octane was used as crosslinking reagent for solidification. Besides, 2 wt% Span 80 was also added to the crosslinking reagent for the stabilization of chitosan emulsion templates. Subsequently, as-synthesized emulsion templates were collected and crosslinked in the

solidification bath, where Schiff-base type chemistries took place between -CHO of glutaraldehyde and -NH_2 of chitosan. Fig. 1b schematically depicts the crosslinking reaction process. CS biosorbents were then thoroughly washed with acetone, ethanol and deionized water successively before the final drying at 40 °C for 3 h.

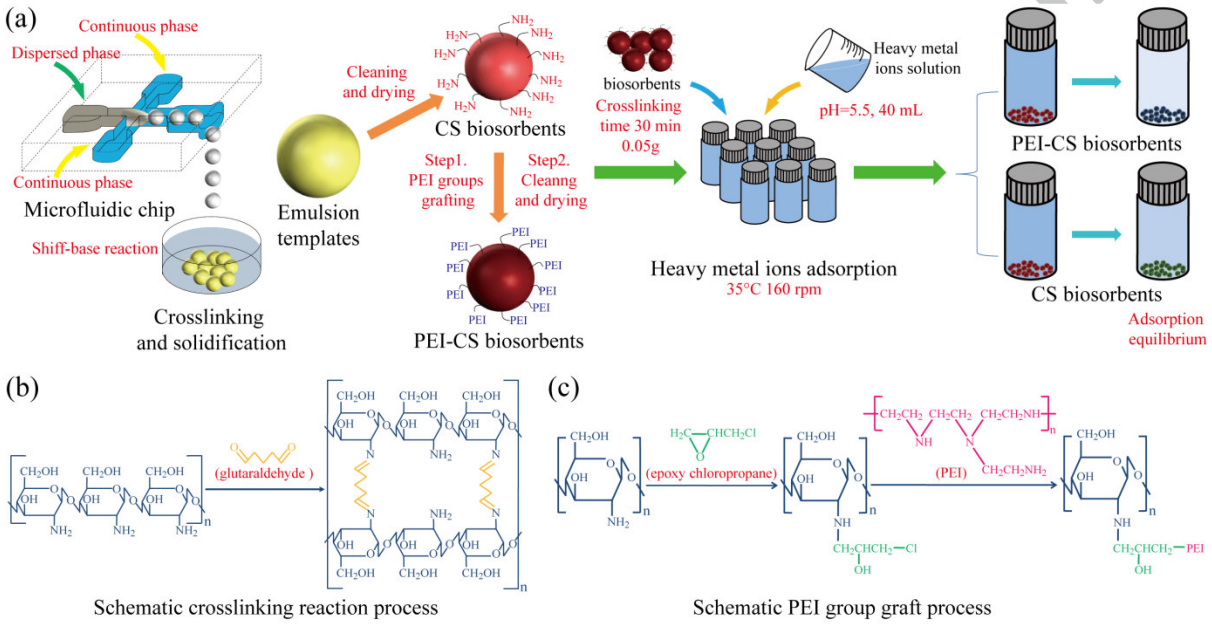

Fig. 1. (a) The overview of the synthesis process of PEI-CS biosorbents and batch adsorption experiments; (b) Schematic crosslinking reaction process; (c) Schematic PEI group graft process.

2.2.2 PEI-CS biosorbents

To synthesize PEI-CS biosorbents, as-prepared CS biosorbents were then grafted with PEI groups by chemical modification processes[43] as shown in Fig. 1a. Meanwhile, Fig. 1c depicts the PEI group graft process. Firstly, as-synthesized CS biosorbents were washed with an aqueous solution containing 50 wt% isopropyl alcohol three times and then suspended in isopropyl alcohol. CS biosorbents were transferred into a beaker containing isopropyl alcohol

with 0.5 wt% epoxy chloropropane. The reaction was carried out at 50 °C for 2 h accompanied by gentle stirring, followed by washing with excess deionized water before being well mixed in 50 wt% PEI aqueous solutions at 80 °C for 3 h under constant stirring. Eventually, PEI-CS biosorbents were thoroughly washed with deionized water and dried at 40 °C for 2 h.

2.3 Material characterization analysis

2.3.1 Optical measurements

The morphology investigation of emulsion templates, CS biosorbents and PEI-CS biosorbents were first carried out using an optical microscope (AZ100, Nikon, Japan). Particle monodispersity was defined utilizing coefficients of variation (CV), which can be calculated according to the following equation:

$$CV = \frac{\left(\sum_{i=1}^{N} \frac{(D_i - \overline{D_n})^2}{(N-1)}\right)^{\frac{1}{2}}}{\overline{D_n}} \times 100\% \quad (1)$$

where D_i is the diameter of each emulsion template or biosorbent and $\overline{D_n}$ is the average diameter of emulsion templates or biosorbents. In this work, same sampling numbers were employed for the two types of biosorbents as 600. Not only the surface, but also the internal structure of the biosorbents were detailed as observed by scanning electron microscope (SEM, HITACHI-S3400N, HITACHI, Japan). To get the composition information of various biosorbents and further exploring the effect of crosslinking degree on their final adsorption capacity, Fourier transform infrared spectroscopy (FTIR, Nicolet 6700, Fisher, USA) was utilized to find out different functional groups and their characteristic peak changes in crosslinking process. The tested wavelengths range was 500 - 4000 cm^{-1}.

2.3.2 Mechanical property tests

Mechanical strength is one of critical parameters of absorbent. In this study, 60 samples of the two types of biosorbents were chosen randomly and then tested individually using a force gauge (HPB, capacity 50 N, Handpi Instruments Co., Ltd, Yueqing, PR China) with increasing static pressure until biosorbents rupture to obtain their average mechanical strengths.

2.3.3 Energy dispersive X-ray spectroscope analysis

PEI-CS biosorbents and CS biosorbents were also analyzed by energy dispersive X-ray spectroscopy (EDX, HITACHI-S3400N, HITACHI, Japan) to reveal the distribution of different elements, such as, Cu, nitrogen (N), sodium (Na), aluminum (Al), *etc*., not only on the surface, but also inside (cross-section) of single biosorbent after adsorption equilibrium.

2.4 Batch adsorption studies

Cu ions (with initial concentration of 400 ppm) were adopted as a model contaminant to study the adsorption performance of the newly developed material (Fig. 1a). In terms of pH effect of aqueous solutions on amine groups protonation, especially for PEI-CS biosorbents rich in amine groups, subsequent adsorption experiments were performed at pH = 5.5 unless otherwise stated (see SI Fig. S3). CS biosorbents without PEI functionalization were also prepared and tested in the adsorption experiments for performance comparison. More experimental details can be found in the SI.

2.5 Desorption experiments

In desorption studies, 0.5 mol L^{-1} or 0.25 mol L^{-1} NaOH solution containing 1.5 wt% EDTA were used as the desorption solution. The desorption experiments were performed in duplicate and described as follow: the biosorbents, obtained after adsorption balance with the

same initial Cu ions concentration of 400 ppm, were firstly filtered from the suspension, rinsed with excess deionized water in order to remove Cu ions not adsorbed on biosorbents, and then placed in the desorption solution with gentle stirring. After entire desorption, the biosorbents were finally washed with excess distilled water before being dried at 40 °C for 2 h.

2.6 Regeneration studies

The biosorbents obtained after desorption procedure were repeated in the same way as that in the adsorption experiments to test their reusability. And the readsorption efficiency (R_E) of the biosorbent can be calculated as follow:

$$\mathrm{R_E} = \frac{\mathrm{q_{R,max}}}{\mathrm{q_{max}}} \times 100\% \quad (2)$$

where $q_{R,max}$ is the maximum adsorption capacity determined by the readsorption experiment. This adsorption-desorption cycle was repeated five times.

3. Results and discussion

3.1 Materials characterization

Optical micrographs of chitosan emulsion templates and as-prepared PEI-CS biosorbents are shown in Fig. 2a and b, respectively. A remarkable size uniformity, high monodispersity and outstanding spherical morphology was presented owing to the advantages of microfluidics technology. The average diameters of chitosan emulsion templates after 30 min crosslinking and as-prepared PEI-CS biosorbents were 940 μm and 378 μm, respectively. The biosorbents shrank during solidification process as a result of water extraction in the presence of *n*-octanol. The monodispersity in as-synthesized emulsion templates and biosorbents were only 0.27 % and 2.3 % (see SI Fig. S2c and d), respectively, considerably lower as compared to those of biosorbents synthesized by conventional methods including

stirring (CV > 10%) and membrane (CV ~ 10%). With a reasonable control of two phase velocities, crosslinking time and drying condition, chitosan emulsion template sizes could be easily adjusted (for details, see SI Fig. S2a and b). Fig. 2c and d compares the surface color of CS biosorbents and PEI-CS biosorbents after adsorption equilibrium. The CS biosorbents (Fig. 2c) turn from reddish brown to dark green, while a layer of light blue powder is found attached on the surface of PEI-CS biosorbents (Fig. 2d), completely different from its initial reddish brown color (Fig. 2b). These findings indicated that different adsorption characteristics were involved for PEI-CS and CS biosorbents.

The material morphologies were further characterized by SEM images. Fig. 2e and f show the surface and inner structures of CS biosorbents, demonstrating their solid spherical structures. Moreover, as shown in Fig. 2g and h, the PEI functionalization process has significantly changed the surface properties and texture of the biosorbents as a layer of obvious attachments on the surface can be observed due to grafting of PEI functional groups. Comparing the surface morphologies of two kinds of biosorbents (Fig. 2e and g), the increased surface roughness of PEI-CS biosorbents may provide more adsorption sites for Cu ions.

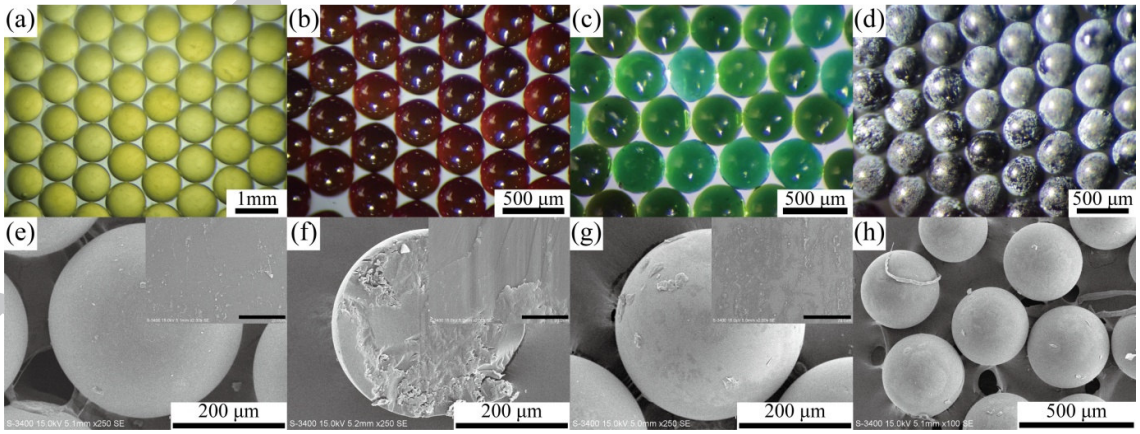

Fig. 2. Optical micrographs of (a) chitosan emulsion templates with crosslinking time 30 min and (b) PEI-CS biosorbents; Optical micrographs of (c) CS biosorbents and (d) PEI-CS biosorbents after adsorption equilibrium; The SEM micrographs of (e) the surface and (f)

inner structures of a CS biosorbent, (g) the surface of a PEI-CS biosorbent and (h) a certain amount of PEI-CS biosorbents. The scale bar of insert images in (e) - (g) is 20 μm.

3.2 Ultra-high adsorption capacity

The adsorption kinetics of Cu ions by CS and PEI-CS biosorbents are compared in Fig. 3a. The final adsorption capacity of PEI-CS biosorbents was 146 mg g^{-1}, which was almost twice as high to those of common CS biosorbents, under otherwise identical sorption conditions. The record-breaking capacity obtained here for PEI-CS biosorbents was also almost triple the performance (52 mg g^{-1}) reported in literature for CS biosorbents[42]. The maximum adsorption capabilities of both natural or artificial adsorbents reported in previous studies under the optimized condition are summarized and compared with as-prepared PEI-CS biosorbents in Table 1. Moreover, PEI-CS biosorbents also showed significantly faster kinetics than CS biosorbents, as it took about only 64 h to reach equilibrium, compared to 144 h for the case of CS biosorbents. It should be mentioned that the saturated adsorption time of as-prepared bisorbents was still longer than the typical saturation time of similar chitosan adsorbents (20 to 100 h) as a result of their non-porous solid spherical structures [42, 44]. The adsorption kinetics of both CS and PEI-CS can be well fitted to pseudo-second order model, since the correlation coefficient (R^2) of both fittings are larger than 0.99. Moreover, the adsorption rate constant k of pseudo-second model was 8.73×10^{-5} g mg^{-1} min^{-1} for PEI-CS biosorbents much larger with respect to those of CS biosorbents (5.96×10^{-5} g mg^{-1} min^{-1}). More details can be found in SI, Table S1.

Table 1 Comparison of maximum adsorption capacity for Cu ions using various adsorbents

Adsorbents	Adsorption capacity (mg g^{-1})	Functional groups	Ref
Nature materials			

Cankırıbentonite (natural clay)	40	NA	[45]
Pomegranate peel	8[a]	NA	[46]
Sunflower stalks	29.3	Coulomb interactions	[47]
Tourmaline	78.86	Electrostatic interactions	[48]
Montmorillonite	4.06[a]	Surface group	[49]
Bamboo charcoals	16.34	Oxygen functional groups	[50]
Granular activated carbon	17	Na	[51]
Palm shell activated carbon	1.581	Sulphate groups	[52]
Graphene oxide (GO)	32	Oxygen functional groups	[53]
Artificial materials			
Nitrogen-functionalized graphene oxide (GO-TETA-MA)	48.64	Amine and oxygen functional groups	[53]
COOH-hybrid carbon nanocomposites	63	Oxygen functional groups	[51]
PVA and carboxymethyl cellulose composite hydrogels	5.5	Hydroxyl and carboxyl groups	[54]
Magnetic cellulose-based beads	47.64	Electrostatic attraction	[55]
Calcium-alginate encapsulated magnetic sorbent	63	Electrostatic attraction	[56]
Thiosalicylhydrazide-poly acrylic acid - coated Fe_3O_4 magnetic nanoparticles	76.9	Amine and sulfur binding sites	[57]
Magnetic calciumalginate/maghemite hydrogel beads	159.24	Carboxylic and amine groups	[58]
Anisotropic layered double hydroxide nanocrystals@carbon nanospheres	19.93	Hydroxyl groups	[59]
Mesoporous titania beads	8.4	Electrostatic attraction	[60]
Functionalized Nature materials			
Chitosan functionalized with 2-pyridinecarboxaldehyde	104.32	Pyridine groups	[61]
Chitosan functionalized with 4-pyridinecarboxaldehyde	45.44	Pyridine groups	[61]
Tartaric acid modified rice husk	31.85	Na	[62]
Chitosan microspheres	52	Amine groups	[42]
Porous chitosan-poly(acrylic acid)-glutaraldehyde microspheres	72	Amine groups	[42]
Electrospun chitosan/polyethylene oxide (PEO) nanofibres	100	Amine groups	[63]
N-(2-Carboxybenzyl) grafted chitosan beads	293	Carboxyl and amine free groups	[64]
CS biosorbents	75.52	Amine groups	This work
PEI-CS biosorbents	145.92	Amine groups	This work

Note: [a] Read from the figures.

Additionally, the adsorption isotherm curves are plotted and fitted them with Langmuir equation in Fig. 3b. The calculated largest adsorption capacities of PEI-CS biosorbents and CS biosorbents were 157 mg g^{-1} and 80 mg g^{-1}, with R^2= 0.990 and 0.998, respectively, also close to the experimental results. All results indicated that the Cu ions adsorption process can be well described by Langmuir's adsorption model. Once the adsorption sites were saturated, the adsorption capacity will not increase anymore.

3.3 High selectivity towards targeted ion

In actual contaminated water, the presence of various metal ions or even soluble chelates can poison the adsorbent. Therefore, selective contaminant removal will be highly important for practical applications. The effect of the presence of different metal ions with various valence states (i.e., Na^+ and Al^{3+}) on Cu^{2+} removal by PEI-CS was subsequently investigated. Na ions and Al ions are of particular interest as they are abundant in natural water sources (such as sea, river and mineral water). The selectivity of CS materials has also been analyzed for comparison.

In the selective adsorption experiment, different conditions of solution were adopted (e.g. 400 ppm Cu^{2+} with 400 ppm Na^+ and/or Al^{3+}; and 100 ppm Cu^{2+} with 400 ppm Na^+ and/or Al^{3+}). Results are shown in Fig. 3c. Generally, both CS-based materials showed good selectivity towards Cu^{2+} adsorption in all cases, in agreement with previous literature reports[42] since the amine groups have good affinity toward Cu ions and can form stable metal chelates. PEI-CS exhibited additionally improved selectivity at the same concentration (400 ppm) of Na^+, Al^{3+} and Cu^{2+} in solution, reaching 94.7 % (much higher than that of CS, 86.8 %). Under more extreme conditions (100 ppm Cu^{2+} *vs.* 400 ppm Na^+ or Al^{3+} in solution), the selectivity of PEI-CS biosorbents towards Cu ions could be still over 83.8 % as compared to 65.7 % for CS.

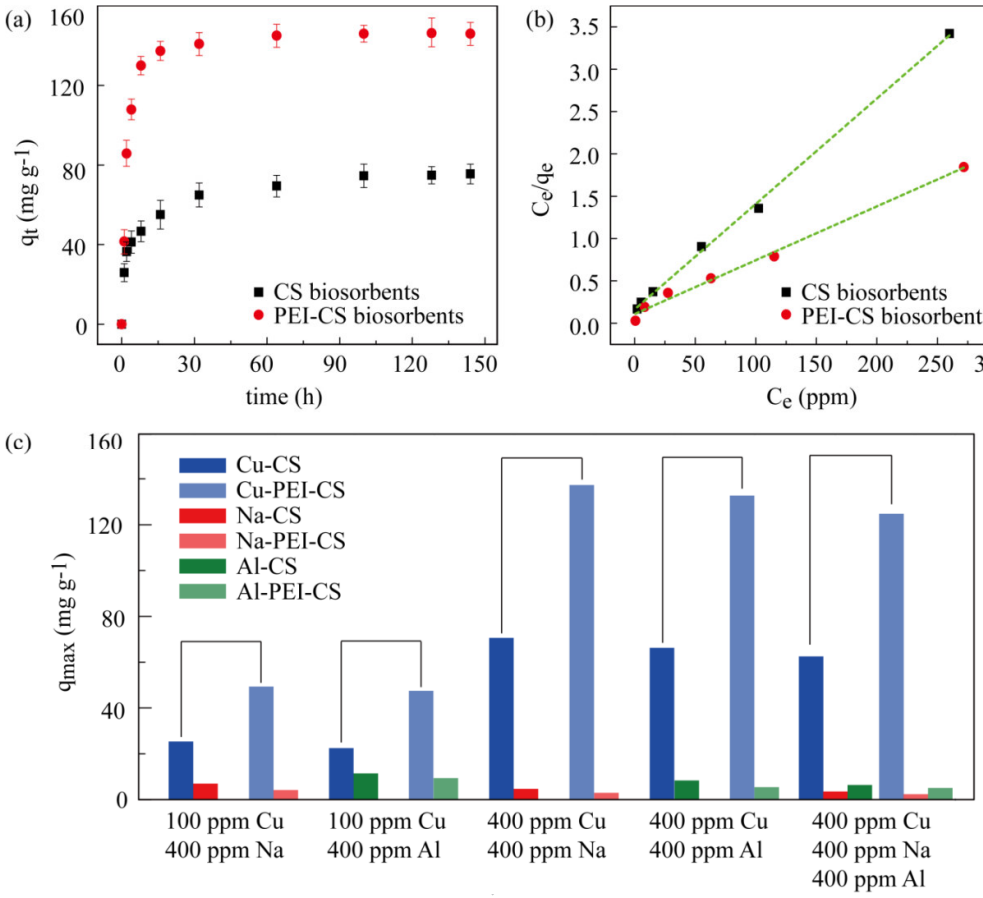

Fig. 3. (a) The typical adsorption kinetics; (b) The linear fitting curves of Langmuir equation; (c) Selective adsorption.

3.4 Mechanical properties

Mechanical strength is another important parameter of absorbents, critical for both the adsorption and separation procedure. For examples, stirring reactors are widely used for accelerated mixing between sorbents and pollutants, while hydro-cyclones are convenient for rapid industrial solid-liquid separation[65]. If the absorbents enriched with toxic metal ions break up in either procedure, it could cause serious secondary pollution. The mechanical strength of as-prepared biosorbents is the capacity to resist external static pressure and remain relatively stable which mainly depends on the crosslinking structure and compactness. Fig. 4a schematically describes the mechanical property test process. We found that clean processes

make a significant difference. CS biosorbents, directly dried after crosslinking without cleaning, turned into powder easily in line with brittle crush regulars. Instead, CS biosorbents subjected to thorough washing exhibited plastic deformation properties, that is, flattening firstly, and then gapped in the most vulnerable position. It is worth mentioning that PEI-CS biosorbents will directly gap while the flattened process was difficult to observe.

The effect of crosslinking degree on mechanical property and adsorption capacity of CS and PEI-CS biosorbents are shown in Fig. 4b and c. It is found that the mechanical strength can be improved with increase in the crosslinking time. However, for CS biosorbent, showing in Fig. 4b, the adsorption capacity will be reduced in the process due to the consumption of amine groups and loss of porous structure. Such trade-off poses a limitation to the enhancement of mechanical strength of the biosorbent by increasing the crosslinking time. On the other hand, the PEI-CS showed better mechanical performance, as a result of multiple factors, including crosslinking degree by reaction, dehydration by n-octanol, and being dried twice in the integrated process. As shown in Fig. 4c, the mechanical strength of PEI-CS biosorbents reaches 0.368 MPa after 60 min crosslinking time. Such value is significantly higher than several natural sorbent materials which normally need additional skeletons in practical industrial processes, and comparable to some commercial engineering polymers (polymeric ionic liquid gel or ion exchange resin, 0.1 MPa - 0.21 MPa). More importantly, the adsorption capacity remained almost unchanged with the increase of crosslinking time, as it was dominated by the amount of grafted PEI groups rather than its crosslink degree.

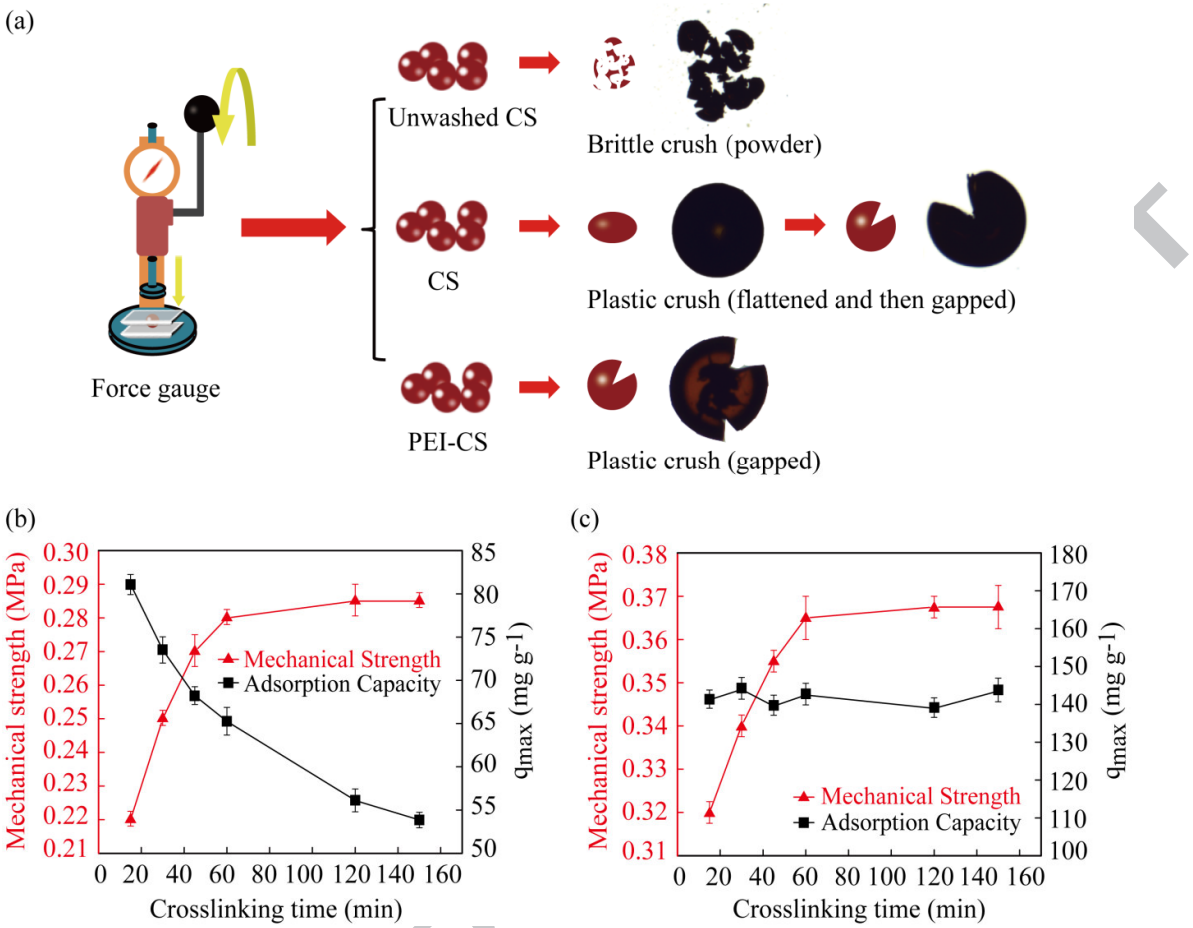

Fig. 4. (a) Schematic mechanical strength tests; The effect of crosslinking degree on mechanical property and adsorption capacity of (b) CS biosorbents and (c) PEI-CS biosorbents.

3.5 Mechanism of adsorption process

In order to explore mechanisms towards ultra-high adsorption properties of the newly developed PEI-CS materials, EDX technology was employed to visualize the elements distribution of Cu on the surface and interior (cross-section) of PEI-CS and CS biosorbents after the adsorption equilibrium (Fig. 5a-d). Here, the Cu element distribution reflects the physicochemical interactions during adsorption and local adsorption capacity within the single particle. It is found that the Cu enrichment intensity is much higher at the PEI-CS

surface than that at CS surface after reaching adsorption equilibrium. It also indicated that different adsorption characteristics were involved. In this regard, the adsorption sites on the surface of PEI-CS biosorbents can be divided into two kinds: the remaining free amine groups on the chitosan molecules after the crosslinking process and the synergy between the remaining amine groups on the chitosan molecules and the additional amine groups provided by PEI groups.

However, the amount of Cu element distributions inside the two types of biosorbents show no significant difference. The results indicated that the PEI-CS biosorbents own better adsorption ability toward Cu ions because of the PEI functional group at the surface, which provides much more adsorption sites for Cu ions chelating. The results were consistent with the N element distribution shown in Fig. S4, representing local amine group density. It also revealed that the surface process dominates the adsorption capacity of PEI-CS biosorbent, and its internal structure showed irrelevance to the performance. All the results confirm that the difference of the adsorption property between two kind of biosorbents can be ascribed to the difference in surface textural properties with various affinity towards Cu ions.

To further analysis the mechanism of high selectivity towards Cu ions for PEI-CS biosorbents, the adsorbed element distributions on the single particle for Na, Al and Cu adsorption processes are comparatively shown in Fig. 5. Compared to Cu, much poorer affinity of Na and Al are observed at the surface of both PEI-CS and CS. Moreover, the response of Na and Al inside the biosorbents can hardly be detected (Fig. 5b3, d3, b4 and d4). It confirms that both the CS and PEI-CS biosorbents show selective adsorption capacity towards Cu in the presence of Na and Al.

From previous analysis, it is confirmed that the amine groups on the CS-based biosorbents showed significant impact on the metal ion adsorption performance. Therefore, it is also important to study the amine group formation mechanism during the synthesis of PEI-

CS materials. Fig. 5e depicts the FTIR spectra of chitosan powder, CS biosorbents and PEI-CS biosorbents, in which the peaks at 3425 cm^{-1} were attributed to the stretching vibration of -OH, -NH, and intermolecular hydrogen bonding, and the peak at 1076 cm^{-1} responded to the stretching vibration of -C-O- in primary and secondary hydroxyl group. It is found that a new peak at around 1654 cm^{-1} related to the introduction of -C=N- was developed during the integrated processes of the CS-based materials, indicating that the Schiff-base reaction between -CHO of glutaraldehyde and $-NH_2$ of chitosan was successful. Moreover, as shown in Fig. 5e, the decreasing intensity of characteristic peaks in the wavenumber range between 1550 and 1750 cm^{-1} indicated that the grafted PEI groups greatly makes up the loss of free amine groups during the crosslinking process, resulting in the enhanced adsorption capacity. Fig. 5f further exhibits the FITR spectrum of CS biosorbents with different crosslinking times in the wavenumber range between 1550 and 1750 cm^{-1}. The characteristic peak of -C=N- continuously declined with the increase in crosslinking time, indicating that the number of free amine groups is significantly reduced. It well explains the reason why the performance of unmodified CS biosorbent decreases with increase in crosslinking time, as shown in Fig. 4b. Such trade-off can be effectively prevented by introducing the new engineering post-processing to produce PEI-CS biosorbents.

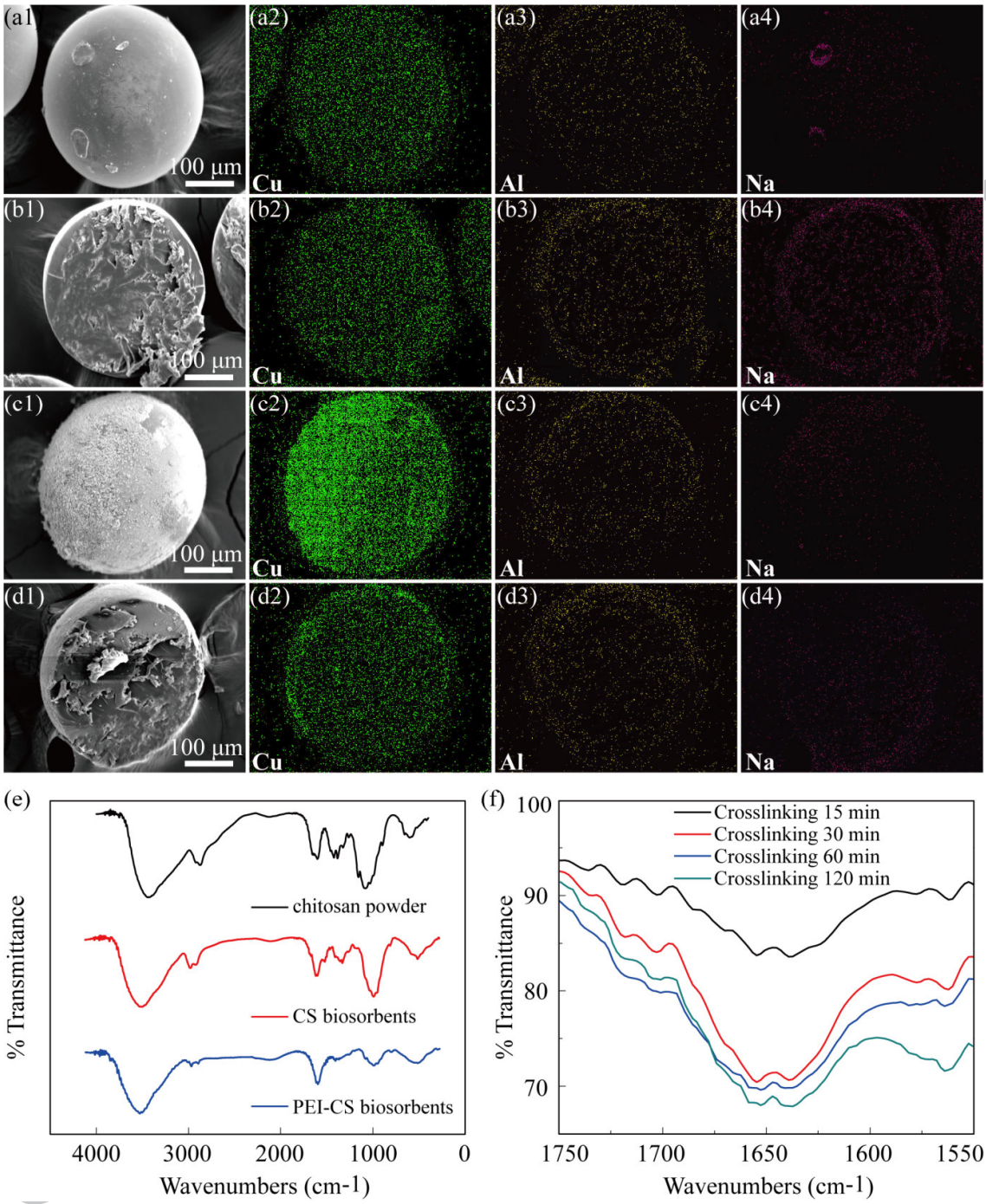

Fig. 5. EDX analysis of (a) the surface and (b) interior of CS biosorbents, and (c) the surface and (d) interior of PEI-CS biosorbents; (e) Comparison of FTIR spectrum of original chitosan powder, CS biosorbents and PEI-CS biosorbents; (f) Local feature of FTIR spectrum of CS biosorbents with different crosslinking times.

3.5 Reusability

For industrial applications, reusability is critical, and is therefore evaluated herein. In our study, desorption was performed in NaOH solution containing 1.5 wt% EDTA. Fig. 6 shows the adsorption-desorption cycle performance of PEI-CS and CS biosorbents in different regeneration conditions. It is found that the NaOH concentration in the desorption process plays a crucial role to determine the readsorbance performance of the PEI-CS biosorbents. Under NaOH concentration of 0.5 mol L^{-1}, R_E of PEI-CS biosorbents decreased dramatically to 48.6 % within 3 cycles, and the readsorption capacity of PEI-CS biosorbents became similar to that of CS biosorbents. It indicates that the PEI functional group at the surface of biosorbents is not stable and will be consumed in alkaline environment with high OH^- concentration. To improve the reusability, the desorption process was then optimized with reduced NaOH concentration at 0.25 mol L^{-1}. Under this condition, the PEI-CS biosorbents show acceptable usability, as the R_E is still higher than 71.2 % after 5 adsorption-desorption cycles, of which the stability was almost comparable with the CS biosorbents (79.7 % R_E at 5^{th} cycle). The results demonstrated that lower OH^- concentration is desired to maintain the reusability of PEI-CS material. Nevertheless, the NaOH concentration cannot be unlimitedly reduced, because a certain level of alkaline environment is needed to completely dissolve EDTA, the vital component of desorption solution. Therefore, although acceptable reusability of PEI-CS material has already been demonstrated, there is still large room to further optimize the desorption process for even higher adsorption-desorption cyclic performance.

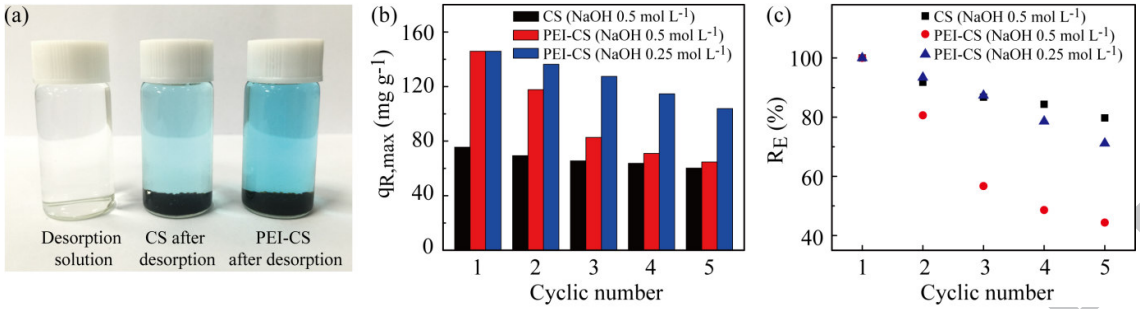

Fig. 6. (a) The color changes of desorption solution after desorption process; (b) Maximum readsorbance and (c) Readsorption efficiency (R_E) of biosorbents for 5 adsorption-desorption circulations.

4. Conclusions

PEI-CS biosorbents with highly monodispersed, good mechanical property, and unparalleled selective adsorption capacity were successfully synthesized by employing facile microfluidics emulsion technology and targeted functional groups modification. The PEI-CS biosorbents were demonstrated to efficiently remove toxic Cu ions from contaminated water and be superior to typical chelating polymer absorbents. Meanwhile, benefiting from great mechanical property, the Cu-loaded biosorbents can be rapidly separated by industrial separation approaches, such as hydro-cyclone, and keep intact and active during the whole procedure. Additionally, the absorbed metal ions could be desorbed in the alkaline EDTA solution in seconds, which is convenient for PEI-CS biosorbents reuse. More importantly, adsorption over PEI-CS biosorbents was found to be highly selective towards Cu ions in the presence of other ions such as Na and Al widely found in nature. Also, the as-prepared biosorbents exhibited good affinity towards other toxic metal ions, including Co ions and Mn ions (for details, see SI, Fig. S5). Benefit from economic and biocompatible substrate materials, coupled with facile synthesis and targeted modification approach, PEI-CS

biosorbents have great promise as an effective potential biosorbent for removal of toxic ions from contaminated water.

Acknowledgements

This work was supported by The National Basic Research Program of China (973 Program, 2014CB748500), National Natural Science Foundation of China (51406057, 51578239, 51322805) and Research Fund for the Doctoral Program of Higher Education of China (20130074120019).

Appendix A. Supplementary data

Supplementary data associated with this article can be found in Supporting Information.

References

[1] R. Martinez-Palou, R. Luque, Applications of ionic liquids in the removal of contaminants from refinery feedstocks: An industrial perspective, Energy & Environmental Science, 7 (2014) 2414-2447.

[2] Y.Y. Guo, H. Guo, Y.P. Wang, L.X. Liu, W.W. Chen, Designed hierarchical MnO2 microspheres assembled from nanofilms for removal of heavy metal ions, RSC Advances, 4 (2014) 14048-14054.

[3] H.Y. Lee, D.R. Bae, J.C. Park, H. Song, W.S. Han, J.H. Jung, A selective fluoroionophore based on BODIPY-functionalized magnetic silica nanoparticles: Removal of Pb^{2+} from human blood, Angewandte Chemie-International Edition, 48 (2009) 1239-1243.

[4] A. Shahbazi, H. Younesi, A. Badiei, Batch and fixed-bed column adsorption of Cu(II), Pb(II) and Cd(II) from aqueous solution onto functionalised SBA-15 mesoporous silica, Canadian Journal of Chemical Engineering, 91 (2013) 739-750.

[5] I. Zawierucha, C. Kozlowski, G. Malina, Immobilized materials for removal of toxic metal ions from surface/groundwaters and aqueous waste streams, Environmental Science-Processes & Impacts, 18 (2016) 429-444.

[6] S.K. Sharma, Heavy metals in water presence, Removal and Safety, UK, 2014.

[7] X. Qiu, N.J. Li, S. Yang, D.Y. Chen, Q.F. Xu, H. Li, J.M. Lu, A new magnetic nanocomposite for selective detection and removal of trace copper ions from water, Journal of Materials Chemistry A, 3 (2015) 1265-1271.

[8] X.B. Wang, X.Y. Ma, Z. Yang, Z. Zhang, J.H. Wen, Z.R. Geng, Z.L. Wang, An NBD-armed tetraaza macrocyclic lysosomal-targeted fluorescent probe for imaging copper(II) ions, Chemical Communications, 49 (2013) 11263-11265.

[9] M. Vafaeezadeh, M.M. Hashemi, N. Ghavidel, Polarity adjustment of a nanosilica-functionalized polyamine modified by ionic liquid for removal of Cu^{2+} from aqueous solutions, RSC Advances, 6 (2016) 14128-14133.

[10] J.L. Huisman, G. Schouten, C. Schultz, Biologically produced sulphide for purification of process streams, effluent treatment and recovery of metals in the metal and mining industry, Hydrometallurgy, 83 (2006) 106-113.

[11] F. Akbal, S. Camci, Copper, chromium and nickel removal from metal plating wastewater by electrocoagulation, Desalination, 269 (2011) 214-222.

[12] M.M. Pendergast, E.M.V. Hoek, A review of water treatment membrane nanotechnologies, Energy & Environmental Science, 4 (2011) 1946-1971.

[13] R. Camarillo, J. Llanos, L. Garcia-Fernandez, A. Perez, P. Canizares, Treatment of copper (II)-loaded aqueous nitrate solutions by polymer enhanced ultrafiltration and electrodeposition, Separation and Purification Technology, 70 (2010) 320-328.

[14] A. Lee, J.W. Elam, S.B. Darling, Membrane materials for water purification: design, development, and application, Environmental Science-Water Research & Technology, 2 (2016) 17-42.

[15] F. Perreault, A.F. de Faria, M. Elimelech, Environmental applications of graphene-based nanomaterials, Chemical Socoity Reviews, 44 (2015) 5861-5896.

[16] W.W. Li, H.Q. Yu, Z. He, Towards sustainable wastewater treatment by using microbial fuel cells-centered technologies, Energy & Environmental Science, 7 (2014) 911-924.

[17] A. Carreon-Alvarez, A. Herrera-Gonzalez, N. Casillas, R. Prado-Ramirez, M. Estarron-Espinosa, V. Soto, W. de la Cruz, M. Barcena-Soto, S. Gomez-Salazar, Cu (II) removal from tequila using an ion-exchange resin, Food Chemistry, 127 (2011) 1503-1509.

[18] Z.D. Wang, Y.T. Feng, X.G. Hao, W. Huang, X.S. Feng, A novel potential-responsive ion exchange film system for heavy metal removal, Journal of Materials Chemistry A, 2 (2014) 10263-10272.

[19] S.M. Lee, A.P. Davis, Removal of Cu(II) and Cd(II) from aqueous solution by seafood processing waste sludge, Water Research, 35 (2001) 534-540.

[20] L. Monser, N. Adhoum, Modified activated carbon for the removal of copper, zinc, chromium and cyanide from wastewater, Separation and Purification Technology, 26 (2002) 137-146.

[21] S.F. Alshahateet, A.G. Jiries, S.A. Al-Trawneh, A.S. Eldouhaibi, M.M. Al-Mahadeen, Kinetic, equilibrium and selectivity studies of heavy metal ions (Pb(II), Co(II), Cu(II), Mn(II), and Zn(II)) removal from water using synthesized C-4-methoxyphenylcalix[4]resorcinarene adsorbent, Desalination and Water Treatment, 57 (2016) 4512-4522.

[22] R.Y. Li, L.B. Zhang, P. Wang, Rational design of nanomaterials for water treatment, Nanoscale, 7 (2015) 17167-17194.

[23] M.X. Tan, Y.N. Sum, J.Y. Ying, Y.G. Zhang, A mesoporous poly-melamine-formaldehyde polymer as a solid sorbent for toxic metal removal, Energy & Environmental Science, 6 (2013) 3254-3259.

[24] K.A. Shroff, V.K. Vaidya, Effect of pre-treatments on the biosorption of chromium (VI) ions by the dead biomass of Rhizopus arrhizus, Journal of Chemical Technology and Biotechnology, 87 (2012) 294-304.

[25] M.A. Barakat, New trends in removing heavy metals from industrial wastewater, Arabian Journal of Chemistry, 4 (2011) 361-377.

[26] M. Rajeswari, P. Agrawal, S. Pavithra, Priya, G.R. Sandhya, G.M. Pavithra, Continuous biosorption of cadmium by Moringa olefera in a packed column, Biotechnology and Bioprocess Engineering, 18 (2013) 321-325.

[27] F.L. Fu, Q. Wang, Removal of heavy metal ions from wastewaters: A review, Journal of Environmental Management, 92 (2011) 407-418.

[28] D. Park, Y.S. Yun, J.M. Park, The Past, present, and future trends of biosorption, Biotechnology and Bioprocess Engineering, 15 (2010) 86-102.

[29] P.Z. Ray, H.J. Shipley, Inorganic nano-adsorbents for the removal of heavy metals and arsenic: a review, RSC Advances, 5 (2015) 29885-29907.

[30] A. Tayyebi, M. Outokesh, Supercritical synthesis of a magnetite-reduced graphene oxide hybrid with enhanced adsorption properties toward cobalt & strontium ions, RSC Advances, 6 (2016) 13898-13913.

[31] M.M. Khin, A.S. Nair, V.J. Babu, R. Murugan, S. Ramakrishna, A review on nanomaterials for environmental remediation, Energy & Environmental Science, 5 (2012) 8075-8109.

[32] R.S.D. Castro, L. Caetano, G. Ferreira, P.M. Padilha, M.J. Saeki, L.F. Zara, M.A.U. Martines, G.R. Castro, Banana peel applied to the solid phase extraction of copper and lead

from river water: Preconcentration of metal ions with a fruit waste, Industrial & Engineering Chemistry Research, 50 (2011) 3446-3451.

[33] C. Shen, Y.J. Wang, J.H. Xu, G.S. Luo, Chitosan supported on porous glass beads as a new green adsorbent for heavy metal recovery, Chemical Engineering Journal, 229 (2013) 217-224.

[34] S. Fujita, N. Sakairi, Water soluble EDTA-linked chitosan as a zwitterionic flocculant for pH sensitive removal of Cu(II) ion, Rsc Advances, 6 (2016) 10385-10392.

[35] V. Chabot, D. Higgins, A.P. Yu, X.C. Xiao, Z.W. Chen, J.J. Zhang, A review of graphene and graphene oxide sponge: material synthesis and applications to energy and the environment, Energy & Environmental Science, 7 (2014) 1564-1596.

[36] H.X. Chang, H.K. Wu, Graphene-based nanocomposites: preparation, functionalization, and energy and environmental applications, Energy & Environmental Science, 6 (2013) 3483-3507.

[37] G. Lian, X. Zhang, S.J. Zhang, D. Liu, D.L. Cui, Q.L. Wang, Controlled fabrication of ultrathin-shell BN hollow spheres with excellent performance in hydrogen storage and wastewater treatment, Energy & Environmental Science, 5 (2012) 7072-7080.

[38] F.Y. Ding, H.B. Deng, Y.M. Du, X.W. Shi, Q. Wang, Emerging chitin and chitosan nanofibrous materials for biomedical applications, Nanoscale, 6 (2014) 9477-9493.

[39] M. Rinaudo, Chitin and chitosan: Properties and applications, Progress in Polymer Science, 31 (2006) 603-632.

[40] W.S. Wan Ngah, L.C. Teong, M.A.K.M. Hanafiah, Adsorption of dyes and heavy metal ions by chitosan composites: A review, Carbohydrate Polymers, 83 (2011) 1446-1456.

[41] J.H. Xu, H. Zhao, W.J. Lan, G.S. Luo, A novel microfluidic approach for monodispersed chitosan microspheres with controllable structures, Advanced Healthcare Materials, 1 (2012) 106-111.

[42] J.H. Xu, X.M. Xu, H. Zhao, G.S. Luo, Microfluidic preparation of chitosan microspheres with enhanced adsorption performance of copper(II), Sensors and Actuators B-Chemical, 183 (2013) 201-210.

[43] C.-Y.J. R. -S. Juang, Equilibrium sorption of copper(II)-ethylenediaminetetraacetic acid chelates onto cross-linked, polyaminated chitosan beads, Industrial & Engineering Chemistry Research 36 (1997) 5403-5409.

[44] Y. Zhu, Z. Bai, W. Luo, B. Wang, L. Zhai, A facile ion imprinted synthesis of selective biosorbent for Cu^{2+} via microfluidic technology, Journal of Chemical Technology & Biotechnology, (2017) DOI: 10.1002/jctb.5193.

[45] S. Veli, B. Alyüz, Adsorption of copper and zinc from aqueous solutions by using natural clay, Journal of Hazardous Materials, 149 (2007) 226-233.

[46] E.-S.Z. El-Ashtoukhy, N.K. Amin, O. Abdelwahab, removal of lead (II) and copper (II) from aqueous solution using pomegranate peel as a new adsorbent, Desalination, 223 (2008) 162-173.

[47] G. Sun, W. Shi, Sunflower Stalks as adsorbents for the removal of metal ions from wastewater, Industrial & Engineering Chemistry Research, 37 (1998) 1324-1328.

[48] K. Jiang, T.-h. Sun, L.-n. Sun, H.-b. Li, Adsorption characteristics of copper, lead, zinc and cadmium ions by tourmaline, Journal of Environmental Sciences, 18 (2006) 1221-1225.

[49] Y.-J. Wang, D.-A. Jia, R.-J. Sun, H.-W. Zhu, D.-M. Zhou, Adsorption and cosorption of tetracycline and copper(II) on montmorillonite as affected by solution pH, Environmental Science & Technology, 42 (2008) 3254-3259.

[50] J. Zhang, Z.-H. Huang, R. Lv, Q.-H. Yang, F. Kang, Effect of growing CNTs onto bamboo charcoals on adsorption of copper ions in aqueous solution, Langmuir, 25 (2009) 269-274.

[51] A.B. Dichiara, M.R. Webber, W.R. Gorman, R.E. Rogers, Removal of copper ions from aqueous solutions via adsorption on carbon nanocomposites, ACS Applied Materials & Interfaces, 7 (2015) 15674-15680.

[52] Y.B. Onundi, A.A. Mamun, M.F. Al Khatib, Y.M. Ahmed, Adsorption of copper, nickel and lead ions from synthetic semiconductor industrial wastewater by palm shell activated carbon, International Journal of Environmental Science & Technology, 7 (2010) 751-758.

[53] K. Zhang, H. Li, X. Xu, H. Yu, Facile and Efficient synthesis of nitrogen-functionalized graphene oxide as a copper adsorbent and its application, Industrial & Engineering Chemistry Research, 55 (2016) 2328-2335.

[54] L.-Y. Wang, M.-J. Wang, Removal of heavy metal ions by poly(vinyl alcohol) and carboxymethyl cellulose composite hydrogels prepared by a freeze–thaw method, ACS Sustainable Chemistry & Engineering, 4 (2016) 2830-2837.

[55] X. Luo, X. Lei, N. Cai, X. Xie, Y. Xue, F. Yu, Removal of heavy metal ions from water by magnetic cellulose-based beads with embedded chemically modified magnetite nanoparticles and activated carbon, ACS Sustainable Chemistry & Engineering, 4 (2016) 3960-3969.

[56] S.-F. Lim, Y.-M. Zheng, S.-W. Zou, J.P. Chen, Characterization of copper adsorption onto an alginate encapsulated magnetic sorbent by a combined FT-IR, XPS, and mathematical modeling study, Environmental Science & Technology, 42 (2008) 2551-2556.

[57] K. Zargoosh, H. Abedini, A. Abdolmaleki, M.R. Molavian, Effective removal of heavy metal ions from industrial wastes using thiosalicylhydrazide-modified magnetic nanoparticles, Industrial & Engineering Chemistry Research, 52 (2013) 14944-14954.

[58] H. Zhu, Y. Fu, R. Jiang, J. Yao, L. Xiao, G. Zeng, Optimization of Copper(II) adsorption onto novel magnetic calcium alginate/maghemite hydrogel beads using response surface methodology, Industrial & Engineering Chemistry Research, 53 (2014) 4059-4066.

[59] J. Gong, T. Liu, X. Wang, X. Hu, L. Zhang, Efficient removal of heavy metal ions from aqueous systems with the assembly of anisotropic layered double hydroxide nanocrystals@carbon nanosphere, Environmental Science & Technology, 45 (2011) 6181-6187.

[60] N. Wu, H. Wei, L. Zhang, Efficient removal of heavy metal ions with biopolymer template synthesized mesoporous titania beads of hundreds of micrometers size, Environmental Science & Technology, 46 (2012) 419-425.

[61] C.A. Rodrigues, M.C.M. Laranjeira, V.T. de Fávere, E. Stadler, Interaction of Cu(II) on N-(2-pyridylmethyl) and N-(4-pyridylmethyl) chitosan, Polymer, 39 (1998) 5121-5126.

[62] K.K. Wong, C.K. Lee, K.S. Low, M.J. Haron, Removal of Cu and Pb from electroplating wastewater using tartaric acid modified rice husk, Process Biochemistry, 39 (2003) 437-445.

[63] I. Lakhdhar, P. Mangin, B. Chabot, Copper (II) ions adsorption from aqueous solutions using electrospun chitosan/peo nanofibres: Effects of process variables and process optimization, Journal of Water Process Engineering, 7 (2015) 295-305.

[64] G.Z. Kyzas, M. Kostoglou, N.K. Lazaridis, D.N. Bikiaris, N-(2-Carboxybenzyl) grafted chitosan as adsorptive agent for simultaneous removal of positively and negatively charged toxic metal ions, Journal of Hazardous Materials, 244–245 (2013) 29-38.

[65] F. Wang, Y. Qiu, P.B. Fu, H.L. Wang, Y.T. Long, Reliable on-site characterization of aromatic compounds adsorbed on porous particles with SERS in a dynamic adsorption-hydrocyclone separation process, Analytical Methods, 6 (2014) 9348-9353.

List of Figures

List of Tables

HIGHLIGHTS

1. A facile microfluidic-based route to fabrication of PEI-CS biosorbents is reported.

2. The PEI-CS biosorbents exhibit outstanding selectivity towards target metal ions in complicated condition.

3. The PEI-CS biosorbents show ultra-high adsorption capacity towards Cu ions up to 146 mg g^{-1}.

4. The mechanical property of as-prepared PEI-CS biosorbents is over 0.34 MPa.

5. The readsorption efficiency is still higher than 71.2 % after 5 adsorption-desorption cycles.